Soft Matter

Accepted Manuscript

This article can be cited before page numbers have been issued, to do this please use: M. D. Sosa, M. L. Martínez Ricci, L. L. Missoni, D. H. Murgida, A. Canneva, N. D'Accorso and R. M. Negri, *Soft Matter*, 2020, DOI: 10.1039/D0SM00738B.

ROYAL SOCIETY OF CHEMISTRY

rsc.li/soft-matter-journal

View Article Online
DOI: 10.1039/D0SM00738B

Liquid-Polymer Triboelectricity: Chemical Mechanisms in the Contact Electrification Process.

Mariana D. Sosa[1], M. Luz Martínez Ricci[1], Leandro L. Missoni[1,2], Daniel H. Murgida[1,2], Antonela Cánneva[3], Norma B. D'Accorso[4,5], R.Martín Negri[1,2*] .

1. Instituto de Química Física de Materiales, Ambiente y Energía (INQUIMAE). Consejo Nacional de Investigaciones Científicas y Técnicas (CONICET)-Universidad de Buenos Aires.
2. Departamento de Química Inorgánica, Analítica y Química Física. Facultad de Ciencias Exactas y Naturales. Universidad de Buenos Aires. Argentina.
3. CONICET. YPF TECNOLOGÍA S. A., Av. Del Petróleo s/n – (Entre 129 y 143) Berisso, Buenos Aires 1925, Argentina.
4. Departamento de Química Orgánica. Facultad de Ciencias Exactas y Naturales. Universidad de Buenos Aires.
5. Centro de Investigaciones en Hidratos de Carbono (CIHIDECAR). CONICET-Universidad de Buenos Aires.

*** Corresponding author:** R.Martín Negri: rmn@qi.fcen.uba.ar.
Address: Ciudad Universitaria, Pabellón II. C1428EGA, Buenos Aires, Argentina.

This article is dedicated to the memory of Dr. Enrique San Román, Full Professor of the Faculty of Exact and Natural Sciences, University of Buenos Aires.

Abstract

The liquid-polymer contact electrification between sliding water drops and the surface of polytetrafluoroethylene (PTFE) was studied as function of pH and ionic strength of the drop as well as ambient relative humidity (RH). The PTFE surface was characterized by SEM, water-contact-angle measurements, FTIR, XPS, and Raman spectroscopy. The charge acquired by the drops was calculated by detecting the transient voltage induced on a specifically designed capacitive sensor. It is shown that water drops become positively charged at pH> pH_{zch} (being pH_{zch} the zero charge point of the polymer), while negatively charged for pH< pH_{zch}. The addition to the water of non-hydrolysable salts (NaCl, $CaCl_2$) decreases the electrical charge induced in the drop. The charge also decreases with increasing RH. These results suggest proton or hydroxyl transfer from the liquid to the hydrophobic polymer surface. A proposed thermodynamic model for the ion transfer process allows explaining the observed effects of RH, pH and ionic strength.

Keywords: Contact Electrification; Hydrophobic Polymers; Ion Transfer; Interfaces; Thermodynamics.

View Article Online
DOI: 10.1039/D0SM00738B

1. Introduction

The generation of electrical charges on the surfaces of two materials when are brought into contact (contact electrification, **CE**) is a well-documented phenomenon[1–5]. In the case of metal-metal, semiconductor-metal or semiconductor-semiconductor contacts, **CE** spontaneously occurs and involves electron transfer from a donor to an acceptor surface, driven by their differences in Fermi levels and work functions. Electron transfer also seems to be the main process when one of the surfaces is a metal and the other an insulating or semiconductor oxide[6,7]. The group of Whitesides reported a series of **CE** studies between polymer microspheres and metals[8–10]. More recently, Kawk *et al* described voltage generation for sliding water drops on graphene[11], while Aji *et al* informed peak voltages larger than 5 V for water drops on MoS_2 surfaces[12].

The situation is very different when the two materials in contact are not metals or semiconductors but polymer-polymer, water-polymer or gas-polymer surfaces. In these cases, a mechanical action is usually required to generate **CE**, such as powerful mutual friction (rubbing) or smooth sliding between surfaces. For instance, Liu&Bard[13] induced electrons on the surface of polytetrafluoroethylene (PTFE) and poly(methyl methacrilate) (PMMA), suggesting that electrons are donated from surface states by mechanical breakage of bonds during rubbing on PMMA, which is consistent with the formation of radicals in PMMA by mechanisms earlier reported by Tatar&Kaptan[14]. Diaz *et al*[15] studied the polymer-polymer contact without rubbing but chemically modifying the surfaces with ion or electron donor groups. Additionally, polymers can be charged not only by contact with another material but applying strong electric fields on its surface. One of these methods is the corona charging, extensively described by Burgo *et al*[16] who observed that low density polyethylene surfaces remain negatively charged in equilibrium after dissipation processes, suggesting adsorption on surface heterogeneities of hydroxyl ions, probably originated from dissociation of water vapour at the surface. This leads to a central issue (still unclear) in the studies involving polymers: whether or not the **CE** in polymers involves ion transfer (mass transfer in the form of molecular ions) or electron transfer. Excellent discussions, arguing for or against both processes in polymer-polymer **CE**, had been reported by several researchers, including pioneer works of the groups of Bard, Whitesides, Galembeck, Yatsuzuka, and Diaz, more recently those of Wang, Helseth, Kim, Butt, and other works cited here and therein[1,2,8–10,13,17–29].

The case of liquid-polymer contact electrification (referred as **LPCE** from now on) is still less studied than the polymer-polymer case and the basic physicochemical aspects have not been clarified yet. The spontaneous generation of electric dipoles and the accumulation of charges during electrical transport across the interface of two media with very different electrical conductivity and polarity is a well-known electromagnetic effect, referred as the Maxwell-Wagner-Sillar (MWS) effect[30–32].

View Article Online
DOI: 10.1039/D0SM00738B

Therefore, the observation of several different electrification processes at the interface between polar liquids and non-polar polymers is not surprising on the bases of the MWS effect, as it has been already mentioned[33]. Recently, Stetten *et al*[21] presented an extensive work of water-drop sliding on a polymer surface, studying the influence of the drop-sliding length and the efficiency of charge-discharge process. The groups of Helseth and Wang made remarkable achievements in the development of energy harvesting devices and self-powered sensors based on **LPCE**[18–20,24,27]. However, the molecular origin of the charge transfer process between a liquid drop and a polymer surface has not been clarified yet. For instance, there is still a lack of systematic work to study correlations between the observed **LPCE** and the physicochemical properties of the liquid media, or with the chemical nature of the polymer. Effects of pH and ionic strength have not been systematically studied, although preliminary works suggest that the **LPCE** efficiency could be dependent on such variables[19,22,28].

Therefore, the objective of the present work is to investigate the molecular origin of contact electrification processes in a liquid-polymer interface, aiming to determine in a quantitative manner the dependence with pH and ionic strength (of the liquid drop) of the charges generated during the **LPCE** between a sliding drop and a fixed polymer surface (PTFE).

2. Materials and Methods

2.1 Chemicals

All solvents and reagents were of analytical quality and used as received. Polyvinylidene fluoride (PVDF) powder (Mr 534,000 $gmol^{-1}$) was purchased from Sigma Aldrich. *N*,*N*-dimethylformamide was purchased from Anedra (Argentina). Water was purified in a MQ filter. PTFE pipes and PTFE powder were from Industrias J&Q (Argentina).

2.2 Instrumentation

Surface morphology was analysed using a Field Emission Scanning Electron Microscope (FESEM; Zeiss Supra 40 Gemini). Infrared spectra (ATR and transmission) were recorded using Nicolet 8700 equipment. Raman spectra were acquired with a confocal LabRAM HR Evolution Raman microscope from Horiba using 532 nm excitation. X-ray photoelectron spectroscopy (XPS) essays were carried out with a SPECS instrument, using a monochromatic AlKα (1486.6 eV) operating at 100W and 10 keV, spot size 3.5 × 1 mm^2. Automatic sample charge neutralization was necessary due to the low conductivity of the samples, which was performed with a FG 15/40. Vacuum chamber pressure was maintained below $<5 \times 10^{-9}$ mbar, and binding energies (BE) referred to adventitious

C1s emission at 285.0 eV. Water Contact Angle (**WCA**) measurements were done in a Rame-hart 200 standard contact angle goniometer with DROPimage standard software.

An oscilloscope Hantek MSO5062D (Internal impedance: 10MΩ) was used for recording the transient voltages on a loading resistance generated by the **LPCE**.

2.3 Device for Water-Polymer Contact Electrification Generation and Detection

Figure 1 shows a scheme of the implemented set-up for **LPCE** studies.

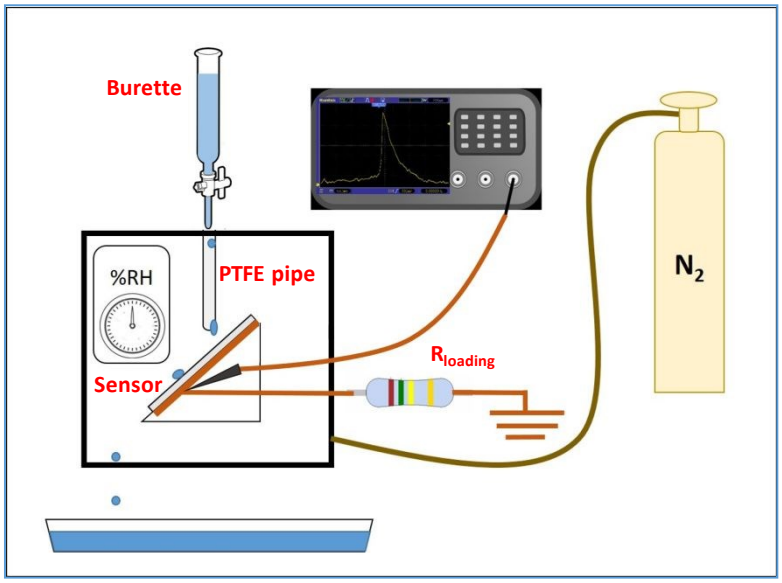

Figure 1. Device for **LPCE** determinations. Liquid drops are delivered from the burette into a PTFE pipe. Afterwards, drops fall on the sensors surface. The metallic substrate of the sensor is connected to ground through a resistance, $R_{loading}$. The oscilloscope detects transient voltages on the resistance.

The core of the device is composed by two elements: a PTFE pipe (where charges are generated) and a sensor (where charges are detected). Liquid drops are vertically delivered from a glass burette into a PTFE pipe at a rate of 72 drops per minute. The volume of the drops is about 0.05 mL. The PTFE pipe, placed vertically, has a length of 20 cm. After sliding along the pipe, drops fall on the surface of the sensor. The PTFE pipe and the surface of the sensor are separated by 1 cm forming an angle of 135 degrees. The sensor component is given by a dielectric polymer film (dimensions: 2x2 cm^2) coated on the surface of a metallic substrate. The electrical charge of the drops was detected by connecting a metal wire to the bottom surface of the metal substrate. This wire is connected to ground through a loading resistance, $R_{loading}$=151 kΩ. The transient voltage on the resistance is detected with the oscilloscope. The PTFE pipe and the sensor are placed inside of an acrylic box where gas nitrogen and/or water vapour was added for changing the ambient humidity. Relative humidity was monitored with a commercial device. All experiments were performed at room temperature (23-25 °C).

View Article Online
DOI: 10.1039/D0SM00738B

2.4 Sensor preparation

The polymer film sensor is prepared in a four-step process which is sketched in **Figure 4:**

Step 1: *Template*: an NAA (Nanoporous Anodic Alumina) film is obtained through an anodization process of commercial 0.8 mm thick aluminium 1050 foil. Prior to the anodization process the aluminium foil is cleaned by immersion in acetone and then thoroughly rinsed with bidistilled water. The sample is anodized at a constant voltage (15 V) for 75 seconds in a 15 % m/v sulphuric acid solution in a homemade PTFE cell with a graphite cathode. The NAA film is then left during 40 minutes in the same acid solution for an opening pore process. Finally, the sample is thoroughly rinsed with bidistilled water.

Step 2: *Polymer deposition:* a polymer mix is formulated with PTFE and PVDF (1 g/10 g). The polymers are dispersed in DMF (3 g DMF/1 g PVDF) by stirring for 1 hour. Then, the mix is kept in ultrasound for 15 minutes. Afterwards, 200 μL of the polymer composite is deposited on the template and after 5 minutes the solvent is evaporated at 120 ºC for 30 minutes.

Step 3: *Polymer removal:* After polymer curing, the polymeric film is mechanically and carefully separated from the AAO template obtaining in the back-side of the PTFE-PVDF film a meso/micro structured film.

Step 4: *Sensor deposition:* To obtain an electrical contact, the PTFE-PVDF film is attached to an Al foil with conductive Ag paint, exposing the rough surface to the air.

3. Results

3.1 PTFE pipe characterization

SEM images of the pipe surface (**Figure 2a**) show sub-micrometric highly compact fibber-like structures. Microscopic models correlate these nano-micro structures to the hydrophobic character of polymer surfaces, which is essential to ensure the rolling of the water drop on the pipe[34-36]. The hydrophobic character of the PTFE pipe surface is confirmed by water-contact-angle determinations (**WCA** ≅ 125 degrees; inset **Figure 2a**). The chemical composition of the pipe surface was spectroscopically studied by Raman, FTIR and XPS, with emphasis on detecting absorbed water and hydroxyl groups, which has been reported for PTFE[37]. The recorded Raman spectra of the pipe surface are in excellent agreement with those previously reported for PTFE[38] (**Figure 2b**).

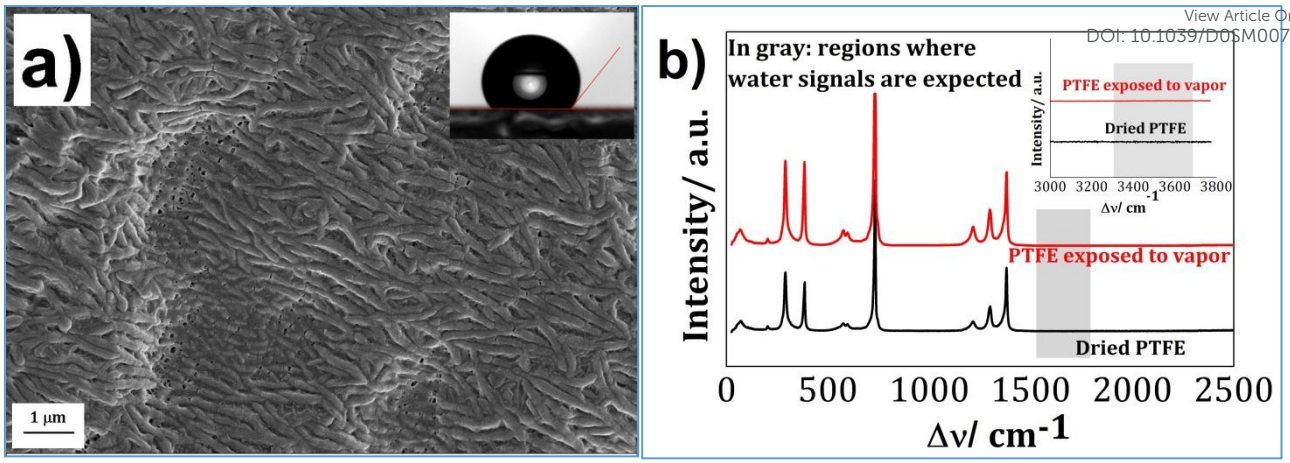

Figure 2. PTFE pipe. a) SEM image. Inset: **WCA** image of the PTFE surface. b) Raman spectra of PTFE surfaces: a *dried* surface (black curve) and a previously exposed to water vapour (*wet* sample, red curve), as indicated in the figure. Inset: 20X amplification.

The adsorption of water and hydroxyl groups on the surfaces of hydrophobic polymers is a well-known phenomenon in polymer science [39,40], and particularly for PTFE surfaces[41]. Therefore, in order to investigate the possible adsorption of water molecules on the pipe surface used in the present work, FTIR and XPS essays were performed in the following conditions:

Condition 1: a sample of the PTFE tube was exposed to water vapours from boiling water for a few minutes. These samples are referred to as the *wet* samples.

Condition 2: a protocol was followed to reduce, as much as possible, the amount of water on the PTFE surface by placing a piece of tube in an oven at 150 °C for 1 hour, then removed and exposed to N_2(g) stream, and finally stored in a silica gel-containing desiccator. These samples are referred to as the *dried* samples.

No differences in the Raman spectra were detected between dried and water vapour-exposed surfaces, probably due to the low sensitivity of Raman spectroscopy to the presence of water (**Figure 2b**). Therefore, XPS and FTIR-ATR experiments were performed in order to compare the *dried* and *wet* samples (**Figure 3**).

View Article Online
DOI: 10.1039/D0SM00738B

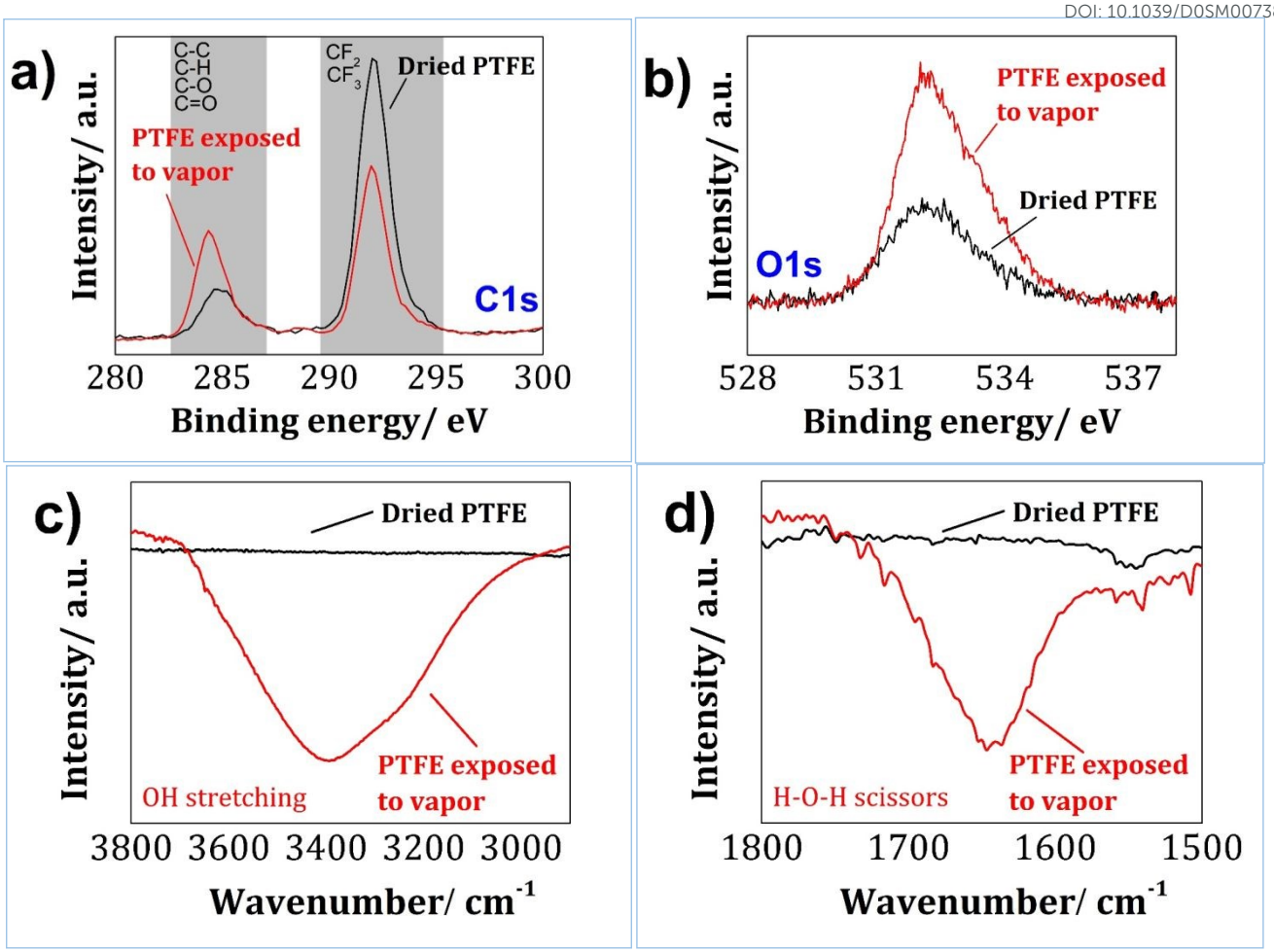

Figure 3. a)-b) XPS-narrow spectra (C1s and O1s) of *dried* (black curves) and *wet* (red) PTFE pipes. c)-d) FTIR-ATR spectra of PTFE surfaces prepared under different conditions. Dried samples (black curves) were previously stored under dried conditions. The red curves correspond to PTFE pipes that were previously exposed to water vapour (red curve), referred as *wet* pipes in the text.

Figure 3a shows C1s XP spectra for the dried and wet samples. Spectra show two signals: a low binding energy peak at about at ~285 eV attributed to organic carbon (aromatic, aliphatic and oxidized) and a the more intense peak at ~292 eV due to $–CF_2$ and $–CF_3$ groups[42,43]. **Figure 3b** shows the O1s XP spectra with a broad band at ~ 532 eV. Both figures show a relative increment of oxygenated species in the *wet* sample. The XPS results clearly show the presence of oxygen species on the PTFE surface.

Analogous features are observed in the infrared spectra: in sharp contrast to *dried* sample, the FTIR-ATR spectra of *wet* PTFE exhibit strong bands at ca. 1640 and 3500 cm^{-1} (**Figures 3c-d**), which are assigned to bending and stretching vibrational modes of water, respectively.

These results lead to a relevant conclusion for **LPCE**: the possibility of finding oxygen species and OH groups on the surface of PTFE.

View Article Online
DOI: 10.1039/D0SM00738B

3.2 Sensor characterization

To optimize the harvesting of charges, a hydrophobic surface sensor is required. For this purpose, we combine two strategies: from one side the use of a hydrophobic polymer mixture (PVDF + PTFE) and from another side, surface structuring. For this last aim, the sensor is prepared in a four step process detailed in Section 2.4. An AAO film over a commercial Al foil is used as template to get a meso/micro final structure. A top-view SEM image of the NAA film is shown next to STEP 1 in **Figure 4**. After the anodization process, the template exhibits a mean size pore diameter of (11 ± 2) nm which assures the meso scale. The micro scale is obtained due to the natural corrugation of the commercial Al foil. The final hierarchical irregular meso/microstructure is observable in the SEM image of the sensor surface next to STEP 4. The image shows nano-protuberances, where it is possible to distinguish the presence of the two polymers used in the formulation (PVDF and PTFE). The **WCA** for the surface is 100 degrees (Inset **Figure 4**), which shows the surface has acquired a sufficient hydrophobic quality for an adequate capture of charges. As a checking process, sensors without this meso/micro corrugation have been synthesized and tested, obtaining a poor signal recollection.

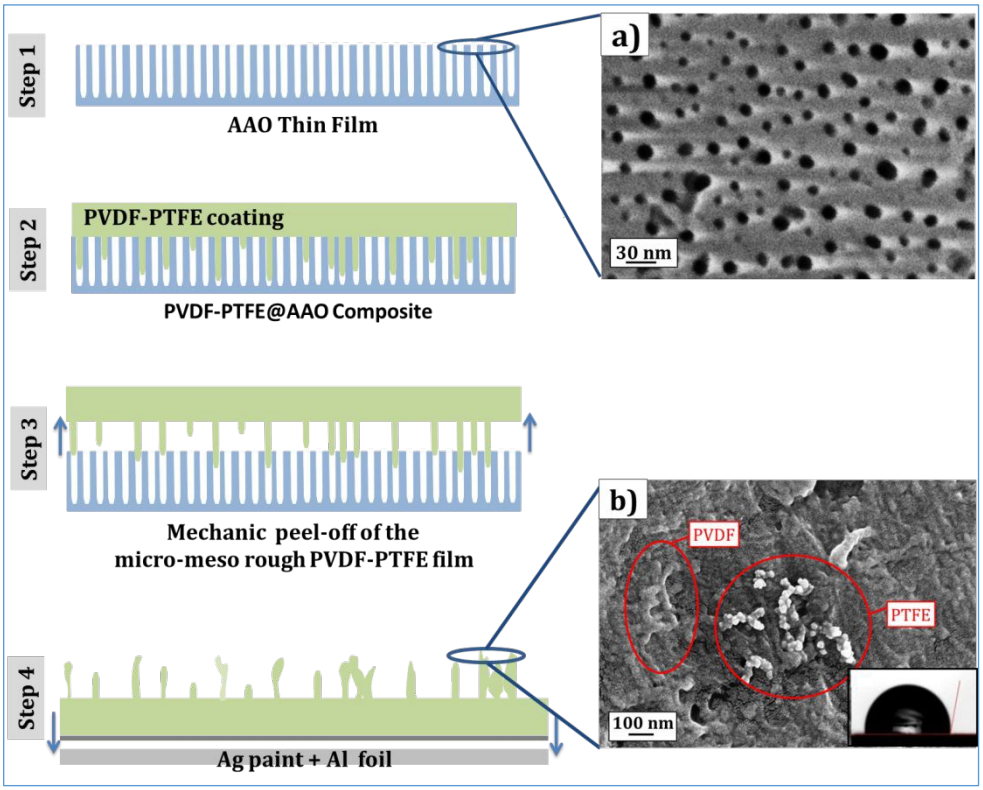

Figure 4. 4-step process to obtain the meso/micro structured sensor. a) NAA template. b) Final PVDF-PTFE polymer sensor. A top-view SEM image of the NAA film is shown while next to STEP 4 it is possible to observe a SEM image of the final sensor surface. Inset: Water-Contact-Angle on the polymer sensor surface.

View Article Online
DOI: 10.1039/D0SM00738B

3.3 Liquid-Polymer Contact Electrification (LPCE) signals

The rise of a voltage transient signal in the oscilloscope each time a water drop touches the sensor points out that the drops are electrically charged (**Figure 5a**). No signals were observed when using drops of toluene or hexane.

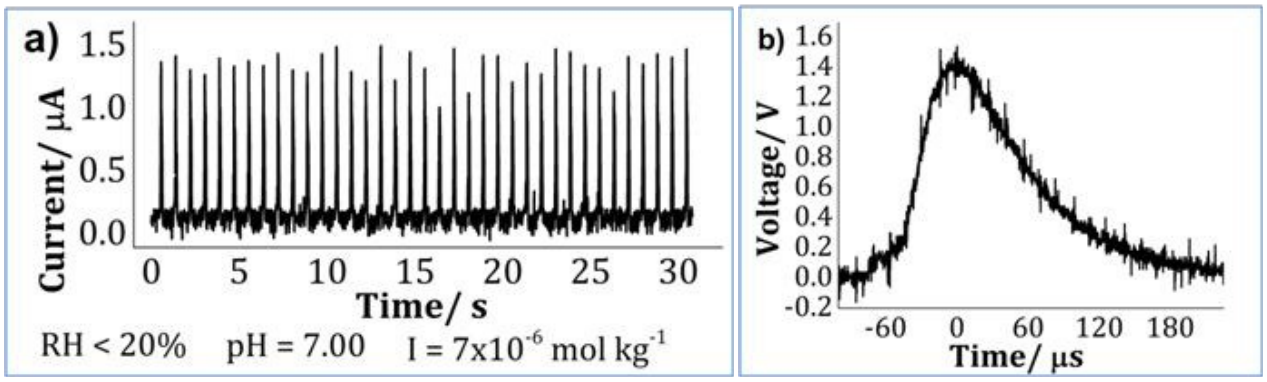

Figure 5. Current and voltage transients. a) Train of pulses originated from delivered water drops at regular frequency (~1 drop s^{-1}). Each peak corresponds to a water drop. b) Zoom of a voltage transient signal, in the scale of microseconds.

A positive transient voltage indicates that the water drop acquires a positive charge when sliding along the pipe, while negative voltages are associated to negative charges. No voltage transient signal was observed when drops are delivered directly from the pipette onto the sensor, without sliding on the PTFE pipe previously. These experiments demonstrate that electrification is generated during the liquid-PTFE contact.

The typical observed transient voltage signal, V(t), is displayed in **Figure 5b**, for the case of pure water. A voltage rise is observed in the oscilloscope when the charged drop touches the surface of the sensor, reaching a peak. This rise is associated to the flow of electrons from ground to the sensor surface, which is required in order to compensate the charge of the drop, keeping electro-neutrality on its surface. Then, the electron flow decreases as charges become balanced and the voltage decays to zero. The rise-decay times are in the order 100 μs. This time scale is much faster than the time it takes to the liquid drop to leave the sensor (in the order of seconds), in agreement with associating the transient signal to electron flow from ground to the surface. Summarizing, the experimental evidence suggests that the transient times are mainly influenced by a charge-discharge mechanism at the sensors surface.

The detected electrical charge, **Q**, is calculated by integration:

$$Q = \frac{1}{R_{loading}} \int_0^{\infty} V(t)dt \qquad [1]$$

where $R_{loading}$ is the resistance between the sensor and ground (see **Figure 1**). The charge **Q** is expected to be proportional to the actual charge acquired by the drop when rolling on the pipe. The difference may arise in several possible neutralization processes of the drop, such as charge exchange with the ambient air.

The influence on **Q** of pH and ionic strength of the water drop, as well as the ambient humidity, is reported in the next sections. The results will let us to analyse the molecular origin of charge electrification processes in a liquid-polymer surface.

3.4 Ambient Humidity Effect

As described in Section 2, the device was placed inside an acrylic box where the relative ambient humidity (RH) was controlled. The voltage transient signals were recorded for different RH at room temperature. **Figure 6a** shows the transients signals for different RH values, where it becomes evident the lowering of the signal when increasing RH. The shape of the transients remains unaffected by RH, as can been seen in **Figure 6b** where an excellent overlap of the signals recorded at different RH is observed when normalizing the transients by the respective value of V_{peak}. No trend with RH was observed for the rise-decay times, which are in the order of 100 μs (no clear trends of the decay times with pH or ionic strength of the drop were observed either).

When analysing the charge according Eq.1, it is observed that **Q** decreases with RH following the tendency of V_{peak}, with important effect for RH > 70 %. **Figure 6c** shows **Q** vs. RH. Excellent experimental reproducibility is obtained at low RH, while the standard deviation σ increases with RH (**Figure 6c**).

These results suggest that the presence of water molecules, protons or hydroxyl groups, which can be induced at large RH, has a detrimental effect on the contact electrification process.

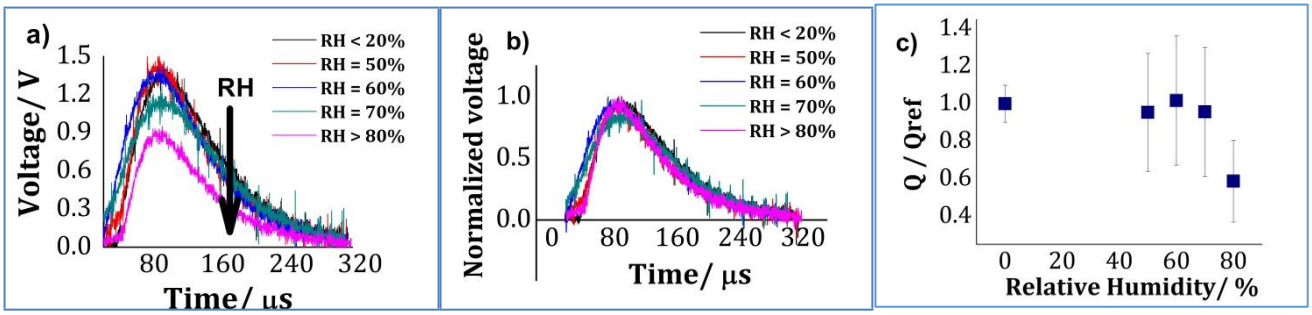

Figure 6. a) Un-normalized transients for different atmospheric relative humidity (RH) b) Normalized transients. c) **Q/Qref** vs RH, where **Q** is the record is the recorded charge and **Q**ref=**Q** at RH<1 %. Each point represents the average on about 20 measurements. The bars represent the standard deviation. No salt added. pH=6.5. T=298 K.

View Article Online
DOI: 10.1039/D0SM00738B

3.5 Effect of pH on LPCE

The pH was changed in the range 1-12 by adding hydrochloric acid (pH < 6.5) or sodium hydroxide (pH > 6.5).

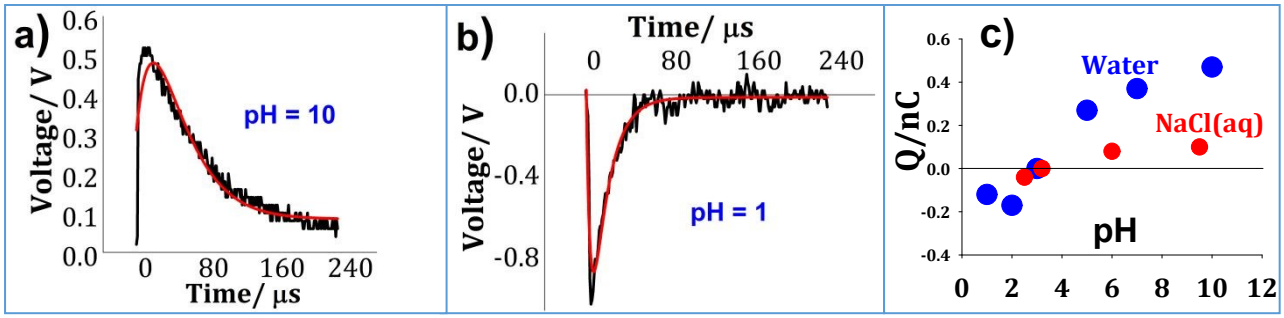

Figure 7. Effect of pH on **LPCE**. a) Positive signal at pH=10. b) Negative transient at pH=1. c) Charge, **Q**, as function of pH. ●:water without salt added. ●:NaCl aqueous solution, 10^{-3} molkg^{-1}.

The water drop acquires negative charge (**Q** < 0) for pH < 3, no charge (**Q** = 0) when pH≅ 3 and positive charge (**Q** > 0) when pH > 3 (**Figure 7**). Moreover, the charge increases with pH (**Figure 7c**). This increase is dependent on the concentration of salts in the drop: the larger salt concentration, the lower variation of **Q** with pH. Remarkably, the pH of zero charge (pH_{zch}), i.e. the pH at which the net charge of a surface is equal to zero, is around 3 independently of the salt concentration (**Figure 7c**). The point of zero charge is polymer specific and is usually determined from measurements of the electrophoretic mobility, which allows determining the z-potential ζ as a function of pH. The value $pH_{zch} \cong 3$ is coincident with the one obtained from determinations of ζ for water-PTFE interfaces[44-46]. Agmon *et al*[47] presented a compilation of literature ζ values for several water/non-polar organic liquid interfaces as a function of pH. Remarkably, ζ = 0 for pH between 2 and 4, irrespective of the chemical nature of the non-polar surface, in agreement with our determination of pH_{zch} = 3 for the water-PTFE interface.

Summarizing, the pH of the drop strongly affects the **LPCE** process, not only by affecting the intensity of the signal but also by changing the sign of the charge acquired by the drop after sliding over the PTFE pipe (**Figure 7**). It is important to remark that the present work shows that determinations of **Q** as a function of pH allow obtaining the point of zero charge of the polymer surface.

View Article Online
DOI: 10.1039/D0SM00738B

3.6 Effect of Ionic Strength on LPCE

The **LPCE** signal decreases when increasing salt concentration (NaCl, $CaCl_2$) in the water drop, as shown in **Figure 8**. In a pioneer work, Yatsuzuka *et al*[22] reported similar results for solutions of NaCl, although no interpretation was proposed.

The decrease of **Q** with salt molality, $\mathbf{m_s}$ (moles of salt per kg of water) is more pronounced for $CaCl_2$ than for NaCl solutions, as expected from the larger ionic strength of $CaCl_2$ at fixed salt concentration. The salts act as quenchers of the **LPCE**, an effect that we observed also in experiments varying pH, as shown in the next section. The results of this section indicate that the chemical composition of the drop has a strong effect on the contact electrification process.

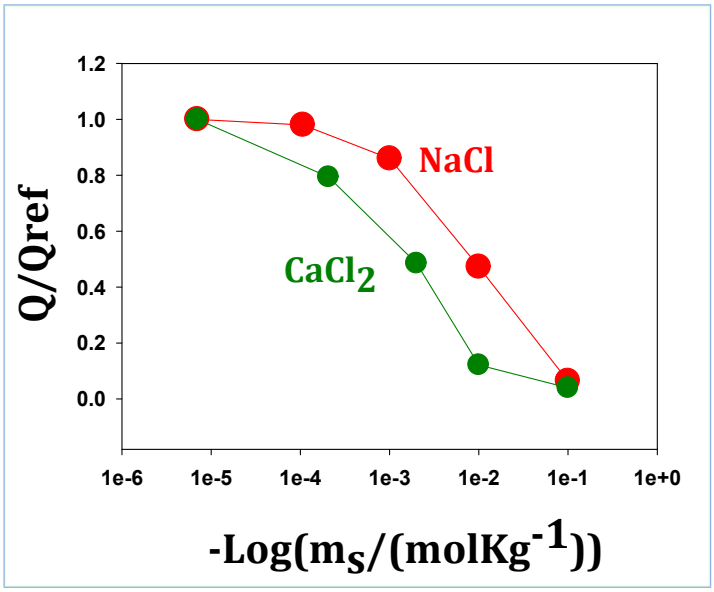

Figure 8. Quenching effect of non-hydrolysable salts on **LPCE**. $\mathbf{m_s}$: salt molality. $\mathbf{Q_{ref}}$ = charge at $\mathbf{m_s}$=7x10^{-7} molkg^{-1}. a)●:NaCl aqueous solution. b)●: $CaCl_2$.aqueous solution. pH=6.5 and T=298 K.

4. Discussion

4.1 General Thermodynamic Model

In this section we present a thermodynamic model for rationalizing the experimental results. The whole experimental evidence suggests the transfer of ions from the liquid drop to PTFE as the origin of **LPCE**, emphasizing the role of water molecules, protons and hydroxyl groups. This hypothesis emerges after analysing the effects of RH, ionic strength and pH described in the previous section, which allows building up a model that assumes hydroxyl (OH^-) and/or proton (H^+) transfer from the liquid drop towards the PTFE surface while the drop slides on the pipe. In agreement with this rationale, we did not observe any transient signals when using drops of toluene and hexane, which do not have the possibility of transferring OH^- or H^+. The experimental results indicate that aqueous

drops with pH > pH_{zch} (≈3 for PTFE) get a positive charge after sliding on PTFE, suggesting OH^- transfer from water to PTFE as the dominant mechanism in this pH regime. On the other hand, $\mathbf{Q} \leq 0$ for pH ≤ pH_{zch} suggests H^+ transfer from the drop to the PTFE at pH < pH_{zch}. In this model, the aqueous drop behaves as a Lewis base at pH > pH_{zch}, transferring OH^- groups to Lewis acid sites on PTFE. Analogously, at pH < pH_{zch} the drop behaves as an acid, transferring H^+ groups to Lewis base sites on the polymer.

The behaviour of water as OH^- or H^+ donor when in contact with a hydrophobic media (mainly at water/oil interface) has been proposed for interpreting experimental results[8,44,46,48] and molecular dynamic simulations[47,49–51]. The acid-base character of the contact electrification is in agreement with the detection of acid-base sites on solid-air surfaces as function of ambient humidity reported by Gouveia *et al*[52] using Kelvin probes.

Although the subject is still controversial, the possibility of ion transfer from water to a hydrophobic media is described in terms of several concatenated interface effects. These effects are related to changes in the hydrogen-bond structure of water because of symmetry breaking at the interface (hence favouring de-attachment of protons and hydroxide groups and its transfer). Clearly, it is not simple to develop a model for H^+ and OH^- transfer incorporating molecular details of O-H bonds at the drop surface in the presence of other ions. Here, a thermodynamic model is proposed.

The proton and hydroxide transfer is formulated as:

$$H_2O(\text{drop surface}) + OH^- \text{ Binding Sites (PTFE)} \rightarrow H^+(\text{drop}) + OH^-\text{-Surface} \quad (pH>pH_{zch}) \quad [2a]$$

$$H_2O(\text{drop surface}) + H^+ \text{ Binding Sites (PTFE)} \rightarrow OH^-(\text{drop}) + H^+\text{-Surface} \quad (pH<pH_{zch}) \quad [2b]$$

Although transfer of OH^- and H^+ is currently mentioned as responsible for the **LPCE** process, no attempts for interpreting the experimental results in terms of a thermodynamic model has been reported as far as we know. Therefore, in this section a thermodynamic model associated to Eq.2 is presented. The **LPCE** process can be related to the change of chemical potential, $\Delta\mu$, associated to ion-transfer (Eq.2) at temperature **T** and pressure **P.** The observed **LPCE** process is spontaneous under the present experimental conditions, then $\Delta\mu \leq 0$. An increase of **Q** (increasing pH, for instance) is associated to an increment in the process spontaneity, therefore $\Delta\mu$ should become more negative. According to Eqs.2a-b, $\Delta\mu$ can be expressed as:

View Article Online
DOI: 10.1039/D0SM00738B

$$\Delta\mu = \Delta\mu^0(T) + RTLn\left(\frac{\left(a^{drop}_{H^+}/a_0\right)\left(a^{polymer}_{OH^-}/a_{0p}\right)}{\left(a^{interface}_{W}/a_{W0}\right)\left(1-\theta^{polymer}_{OH^-}\right)}\right) \qquad \text{at pH} > \text{pH}_{zch} \qquad [3a]$$

$$\Delta\mu = \Delta\mu^0(T) + RTLn\left(\frac{\left(a^{drop}_{OH^-}/a_0\right)\left(a^{polymer}_{H^+}/a_{0p}\right)}{\left(a^{interface}_{W}/a_{W0}\right)\left(1-\theta^{polymer}_{H^+}\right)}\right) \qquad \text{at pH} < \text{pH}_{zch} \qquad [3b]$$

$$\Delta\mu = 0 \qquad \text{at pH} = \text{pH}_{zch} \qquad [3c]$$

where R is the universal constant for gases and $\Delta\mu^0$ the change of chemical potential in the reference standard state at the temperature **T**. The variable $a^{interface}_{W}$ is the water activity at the water-polymer interface. The parameters $\theta^{polymer}_{OH^-}$ and $\theta^{polymer}_{H^+}$ are the fraction of surface adsorption sites covered by OH^- and H^+ groups, respectively, while $a^{polymer}_{OH^-}$ and $a^{polymer}_{H^+}$ are their activities at the polymer surface. The activities a_0, a_{0p} and a_{W0} are the respective activities in the reference state for ionic species in the drop, in the polymer and for water in the drop, respectively (a_0=moldm^{-3}, a_{0p}=moldm^{-2}, a_{W0}=molkg^{-1}).

An additional term, FV_J, should be added to the expression of Δμ in Eqs.3a-b, in order to account for the rise of a junction potential, V_J, during the liquid-polymer contact (which can be different for the cases of OH^- or H^+ transfer). We assume that in the case of the sliding drop, the variations of V_J with pH and ionic strength is a second order effect, hence $V_J = 0$ is taken from now on.

In Eqs.3 $a^{drop}_{H^+}$ and $a^{drop}_{OH^-}$ are the proton and hydroxyl activities in the liquid drop, respectively, which (assuming no difference of activity between surface and bulk in the drop) are related to the pH of the drop. The increase of H^+ or OH^- moles in the drop that arrives to the sensor after leaving the pipe, Δn^{drop}, can be estimated from determinations of the charge, since $\Delta n^{drop} \le \frac{|Q|}{F}$, where F is the Faraday´s constant. With **Q** ~ 0.1-1 nC, then $\Delta n^{drop} \le 10^{-15}$-$10^{-14}$ moles. Therefore, the amount

of transferred charge during the **LPCE** process is too small to induce measurable pH changes in the drop. Since the change of ion concentration, given by Δn^{drop}, is negligible then: (expressing the concentration of H^+ and OH- in moles per cubic decimetres in the drop)

$$\frac{a_{H^+}^{drop}}{a_0} \cong 10^{-pH} \quad [4a]$$

$$\frac{a_{OH^-}^{drop}}{a_0} \cong 10^{-(14-pH)} \quad [4b]$$

Therefore:

$$\Delta\mu = \Delta\mu^0(T) + 2.3RT\left(-pH + \left(Log\left(\frac{a_{OH^-}^{polymer}/a_{0p}}{\left(1-\theta_{OH^-}^{polymer}\right)}\right) - Log\left(a_W^{interface}/a_{W0}\right)\right)\right) \quad \text{pH>pH}_{zch} \quad [5a]$$

$$\Delta\mu = \Delta\mu^0(T) + 2.3RT\left(-(14-pH) + Log\left(\frac{a_{H^+}^{polymer}/a_{0p}}{\left(1-\theta_{H^+}^{polymer}\right)}\right) - Log\left(a_W^{interface}/a_{W0}\right)\right) \quad \text{pH<pH}_{zch} \quad [5b]$$

Note that Eq. 5 relates Δμ with the concentration of ionic species in the liquid drop through the respective activities. Hence, in order to perform quantitative predictions, it is necessary to relate Δμ with the detected charge **Q**. It must be noted that the model is based on a formal chemical reaction associated to the OH^- or H^+ transfer (Equation 2), where the charge acquired by the water drop, referred as $\mathbf{Q_0}$, is exactly the opposite of the charge accepted by the polymer ($-\mathbf{Q_0}$). Here, Δμ is equal to minus the maximum possible non-volumetric work ($-W_{max}$) per mol of transferred ions, Δn^{drop}. In the present case W_{max} is the maximum electrical work that can be delivered by the "charged drop-charged polymer" system. Our approach is to take into account the generation of $\mathbf{Q_0}$ in the drop by considering not a diffuse double layer but a compact single layer (analogous to the Stern-layer model for electrolyte-electrode systems[53]). This hypothesis is based on considering that the OH^- or H^+ transfer must occur within a thin layer at the drop surface. In this picture W_{max} is equal to the

electrical energy stored in the Stern-layer capacitance (C_0), given by $W_{electmax} = \frac{Q_0^2}{2C}$, and the thermodynamics predicts $\Delta\mu = -\frac{FQ_0}{2C_0}$. On the other hand, the charge of the drop when it leaves the polymer surface after sliding, referred as **Q**, was experimentally determined by integrating the recorded current as a function of time, without any assumption or using any model. Concerning the polymer-air interface, the charge on the polymer surface, after the drop leaves the surface, could be different to the charge of the drop because of charge recombination processes at the involved interfaces (water-polymer, water-air and polymer-air), as recently described by Stetten *et al*[21]. Within the context of the presented model, we assume, as a first approximation to a complex problem, that the charge $\mathbf{Q_0}$ introduced in the formalism is proportional to the recorded charge, **Q**. The difference between **Q** and $\mathbf{Q_0}$ is taken into account in the model equations by introducing an effective capacitance, C_{eff}, such as $\mathbf{Q_0}/C_0 = \mathbf{Q}/C_{eff}$. The effective capacitance C_{eff} depends on instrumental factors, microscopic details of the surface (roughness, porosity, etc.) and, in principle, on pH and ionic strength of the water drop.

Therefore, the following expression for Δμ is assumed:

$$\Delta\mu = -\frac{|W_{\max}|}{\Delta n} = -\frac{\left(\frac{Q^2}{2C_{eff}}\right)}{\left(\frac{|Q|}{F}\right)} = -\frac{F|Q|}{2C_{eff}} \qquad \text{(Stern-compact layer)} \qquad [6]$$

The relevance of Eq.6 is given by two aspects: i) Δμ is proportional to an experimentally determined magnitude (**Q**), and ii) Δμ can be related to the chemical composition of the liquid drop and the PTFE surface. By combining Eqs.5 and 6 it is possible to rationalize the effects of pH and ionic strength on **LPCE**, as presented in the next sections.

In a pioneer work, Yates *et al* [54] reported a thermodynamic site-binding model for the adsorption of ionic species (including H^+ and OH^-) of a solution in contact with an electrode, which can be extended to any surface. The authors proposed a situation of electrochemical equilibrium with $\Delta\mu_{electrochemical} = 0$, where (for the case of OH^- adsorption) $\Delta\mu_{electrochemical} = \Delta\mu - F\psi_0$, with ψ_0 the potential difference between the polymer surface and the bulk solution (ψ_0<0 for OH^-

View Article Online
DOI: 10.1039/D0SM00738B

adsorption). This is mathematically equivalent to the approach presented here, where $\Delta\mu = -\frac{|W_{max}|}{\Delta n}$ is proposed, since $F\psi_0 = -\frac{|W_{max}|}{\Delta n}$. It must be noted that the model presented here is a site-binding model also, but while Yates *et al* used a detailed description of the double-layer for recovering ψ_0 as function of pH and ionic strength, we adopt a more simple description which allows to obtain a direct expression for relating $\Delta\mu$ with the detected charge **Q**. This simple analysis presents the drawback of losing accuracy at large ion concentrations or extreme pHs, where a detailed description of the double layer formed in the water drop may be required.

Concerning the ambient humidity effect on **LPCE**, the mechanism of OH^- or H^+ transfer towards free adsorption sites in the polymer, expressed in Eqs.2, is in agreement with the observed decrease of **Q** with RH at large RH. When ambient humidity increases, adsorption sites on the surface of the polymer are occupied with species of oxygen and hydroxides, as observed by XPS and FTIR. Therefore, there will be fewer sites available for the adsorption of OH^- or H^+ from the water drop when it contacts the polymer. In thermodynamic terms, the parameters $\theta_{OH^-}^{polymer}$ and $\theta_{H^+}^{polymer}$ increase with RH. Furthermore, since there is a higher surface concentration of OH^- and H^+ in the polymer due to the ambient humidity, the activities $a_{OH-}^{polymer}$ and $a_{H^+}^{polymer}$ increase with RH. Hence, the increase of $\theta_{ion}^{polymer}$ and a_{ion}^{drop} with RH, determine that $\left(\frac{a_{ion}^{polymer}}{\left(1-\theta_{ion}^{polymer}\right)}\right)$ in Eq.5 increases with RH (ion = OH^- or H^+, depending on pH). It must be noted that all possible departures from ideality due to ion-ion interactions at the polymer surface can be assumed as negligible. In fact, the surface charge density induced on the polymer surface, σ_0, can be roughly estimated by $\sigma_0 \sim$ **Q**/*S*, where *S* is the surface of the water drop in contact with the polymer. Considering **Q** ~ 0.5 nC and *S* ~ 0.2 cm^2 (for a water drop of 50 µL), then σ_0 ~ 1 $nCcm^{-2}$ is obtained, that correspond to molar surface density (σ_0/F) ~ 10^{-14} $molcm^{-2}$ of OH^- or H^+ adsorbed (as indicated before), which is too low for inducing non-ideality effects.

Therefore, Eq.5 predicts Δμ to increase (becomes less negative) when increasing RH and thus **Q** in Eq. 6 is expected to decrease, as it was experimentally observed (**Figure 6**). Hence, the model is in concordance with the observed decrease of the **LPCE** signals with RH.

4.2 Modelling the effect of pH

The Eq.6 is expected to provide more realistic predictions for experiments performed at low ionic strengths, otherwise effects associated to ion-interactions and diffuse double-layer effects, beyond the compact Stern layer model, should be incorporated. Thus, the model was used to analyse the pH effects under moderated ionic strength. Equations 5a-b can be compactly expressed in a single equation by using Eq.6 and imposing the condition **Q** = 0 at pH = pH_{zch}:

$$Q = \frac{4.6RTC_{eff}}{F}\left(\left| pH - pH_{zch} \right| + Log\left(\frac{a_W^{interface}}{a_{Wzch}^{interface}} \right) - Log\left(\frac{B_{ion}^{polymer}}{B_{ionzch}^{polymer}} \right) \right) \quad [7]$$

$$B_{ion}^{polymer} \equiv \frac{a_{ion}^{polymer}}{\left(1 - \theta_{ion}^{polymer} \right)} \quad [8]$$

where "ion" stands for OH^- (at pH > pH_{zch}) and for H^+ (at pH < pH_{zch}). The parameters $a_{Wzch}^{interface}$ and $B_{ionzch}^{polymer}$ are the values of $a_W^{interface}$ and $B_{ion}^{polymer}$ at pH = pH_{zch} , respectively.

Eq. 7 predicts a linear dependence of **Q** with pH, with **Q** = 0 at pH = pH_{zch}. Departures from linearity may be due to saturation of adsorption sites for the transferred ion at the extreme pHs, an effect which is incorporated into the model through the parameters $B_{OH^-}^{polymer}$ (at pH>pH_{zch}) and $B_{H^+}^{polymer}$ (at pH< pH_{zch}). The experimental results of **Figure 7** are in reasonable agreement with a linear dependence of **Q** with pH at moderate pH and departures at the extremes, and recovering pH_{zch} =3 in absence and presence of an added salt.

Fits of Eq.7 to the experimental data indicate also a decrease of the effective capacitance with salt concentration. The following values were recovered from the fits: C_{eff} = 0.7 nCV^{-1} for [NaCl] = 0 and C_{eff} = 0.15 nCV^{-1} for [NaCl] = 10^{-3}M (**Figure 9a**). These values of C_{eff} are in good agreement

View Article Online
DOI: 10.1039/D0SM00738B

with values of capacitance for water-PTFE in the order of 10^{-1} nF reported by Stetten *et al.*[21] using a different methodology.

The driving force of the process is the OH^- concentration (at pH > pH_{zch}) or H^+ concentration (at pH < pH_{zch}), which is expressed through the dependence of **Q** and Δμ with $|pH - pH_{zch}|$. The predicted change of chemical potential in the absence of added acid, base and salt (pH ≅ 6.5) can be estimated from the measured charge **Q** in these conditions, since $\Delta\mu \cong -\frac{Q}{2C_{eff}} \cong -24\text{kJmol}^{-1} \cong -10RT$.

4.3 Modelling the ionic strength effect

Surface effects on water activity are predicted to be of high relevance[47,55], and a rigorous analysis of ionic strength influence on $a_W^{interface}$ requires an approach at molecular level. Nevertheless, the present model provides good qualitative and quantitative agreement with the experiments, following simple phenomenological arguments.

When a non-hydrolysed salt is added to an aqueous solution, the water molecules participate in the solvation of cations and anions (solvation water), decreasing $a_W^{interface}$. This effect is expected to be more pronounced at the drop surface than in bulk, because of the lower number of involved water molecules. Consistently, Eq.5 predicts an increase of Δμ when adding the salt (Δμ becomes less negative), decreasing the spontaneity of the OH^- or H^+ transfer and predicting a decrease of **Q**, as experimentally observed.

Moreover, a phenomenological approach to the surface solvation effects provides excellent quantitative predictions also. The solvation effect can be described as a dynamic equilibrium at the drop surface between free water and solvation water. The involved mathematics is the same that used for Langmuir adsorption-desorption competition for active sites at a surface (where the salt decreases the fraction of water active sites), or equivalently, for static quenching of free water molecules (where the salt acts a quencher). This equilibrium processes at the drop surface is mathematically described by:

Surface Free Water + Salt $\xleftrightarrow{K_{eq}}$ Solvation Complex, where $K_{eq} \equiv \frac{a_{SolvationComplex}}{\left(a_W^{interface}\right)m_S}$ is the equilibrium constant and $a_{SolvationComplex}$ is the activity of the solvated cations and anions.

The balance between free and solvation water is given by $a_W^{interface,pure} = a_w^{interface} + a_{SolvatingComplex}$ (assuming activities=concentrations) where $a_W^{interface,pure}$ is the water activity at the interface in absence of salt. Combining the balance relationship and the equilibrium constant, the following expression is obtained:

$$a_W^{interface} = \frac{a_W^{interface,\,pure}}{\left(1 + K_{eq} m_S\right)} \qquad [9]$$

Introducing Eq.9 into Eq.7, the following relationship is obtained between **Q** and $\mathbf{m_s}$:

$$\frac{Q}{Q_{ref}} = 1 - ALog\left(1 + K_{eq} m_S\right) \qquad [10]$$

where Q_{ref} is the charge generated when using diluted solutions, $\mathbf{m_s} \rightarrow 0$, and A is a constant accounting for all the proportionality factors.

Excellent fits of **Q** vs. $\mathbf{m_s}$ using Eq. 10 are obtained for NaCl solutions with $K_{eq} = (1.25 \pm 0.04)10^3$ $mol^{-1}kg$, $A = (0.45 \pm 0.02)$ (NaCl, **Figure 9b**). In the case of $CaCl_2$, fit is still acceptable, although K_{eq} was recovered with large error: $K_{eq} = (3 \pm 3)10^4$ $mol^{-1}kg$, $A = (0.30 \pm 0.03)$ ($CaCl_2$, **Figure 9c**). In spite of the error, the recovered value of K_{eq} is larger for $CaCl_2$ than for NaCl, as expected from the larger charge of the Ca^{+2} cation. In both cases, the high recovered values of K_{eq} indicates strong solvation effects of the salt on the water molecules at the surface. Summarizing, the developed model provides a very good quantitative prediction of the experimentally observed tendencies of **Q** with salt concentration at fixed pH.

View Article Online
DOI: 10.1039/D0SM00738B

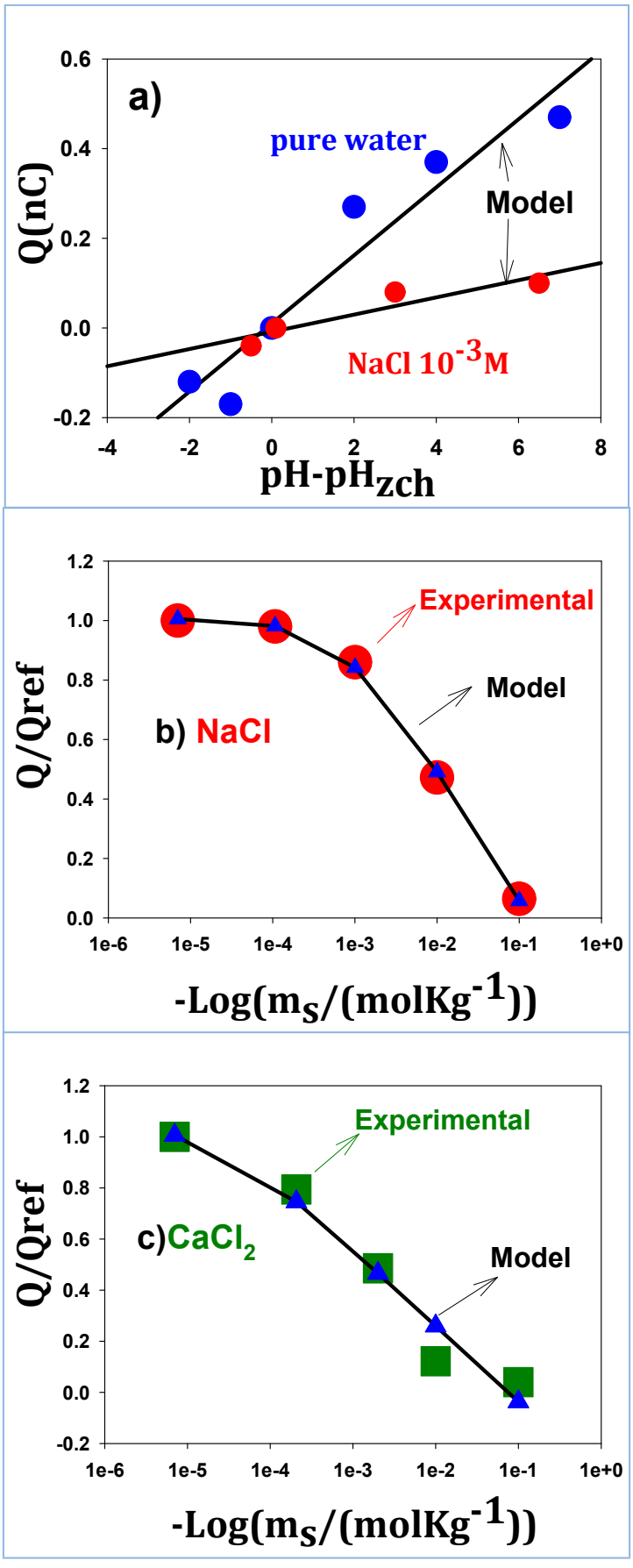

Figure 9. Experimental results versus model predictions. a) Model predictions (straight lines) for pH effects (pH_{zch}=3).b)-c) Model predictions for NaCl and $CaCl_2$ solutions (pH=6.5,T=298K, RH=50%).

View Article Online
DOI: 10.1039/D0SM00738B

5. Conclusions

The experimental results are consistent with the transfer of hydroxyl groups or protons from the water drops to the surface of the polymer. While other possible mechanisms, such as electron transfer, cannot be ruled out, the ion transfer model allows for a consistent interpretation of the data based on simple thermodynamic considerations. This formalism, accounts for the observed effects of ambient humidity, pH and ionic strength of the water droplets. Moreover, it allows obtaining the pH of zero charge of the polymer, the effective capacity of the ion transfer layer and the changes in chemical potential associated with it.

The thermodynamic model presented in this work makes quantitative predictions for the effects of pH and ionic strength of the water drop on the **LPCE** process.

6. Acknowledgments

DHM, AC, MLMR, NBD and RMN are research members of the National Council of Research and Technology (CONICET, Argentina). MS and LM are doctoral students at the University of Buenos Aires (UBA) and recipient of doctoral fellowships from CONICET. Financial support was received from UBA (UBACyT projects 20020150100079BA and 20020170200298BA), Ministry of Science, Technology and Innovations (MINCYT- FONCYT, Argentina, PICT 2011-0377, and Bilateral Project CONICET-SNSF (Swiss National Science Foundation, Switzerland, Res. CONICET 1084/17). The authors acknowledge to Drs. Damián Scherlis and Yamila Perez Sirkin (INQUIMAE, UBA-CONICET) for discussions on computational simulations of water interfaces. RMN thanks to Claudia V. Méndez (E.N.E.T. 27, Argentina) for appreciated help and discussions during COV-19 quarantine.

7. References

1 Z. L. Wang and A. C. Wang, *Materials Today*, 2019, **30**, 34–51.
2 F. Galembeck, T. A. L. Burgo, L. B. S. Balestrin, R. F. Gouveia, C. A. Silva and A. Galembeck, *RSC Adv.*, 2014, **4**, 64280–64298.
3 M. W. Williams, *AIP Advances*, 2012, **2**, 10701.
4 J. Haeberle, A. Schella, M. Sperl, M. Schröter and P. Born, *Soft Matter*, 2018, **14**, 4987–4995.
5 A. Schella, S. Herminghaus and M. Schröter, *Soft Matter*, 2017, **13**, 394–401.
6 Y. S. Zhou, Y. Liu, G. Zhu, Z.-H. Lin, C. Pan, Q. Jing and Z. L. Wang, *Nano Letters*, 2013, **13**, 2771–2776.
7 Y. S. Zhou, S. Wang, Y. Yang, G. Zhu, S. Niu, Z.-H. Lin, Y. Liu and Z. L. Wang, *Nano Letters*, 2014, **14**, 1567–1572.
8 L. S. McCarty and G. M. Whitesides, *Angewandte Chemie International Edition*, 2008, **47**, 2188–2207.
9 B. A. Grzybowski, A. Winkleman, J. A. Wiles, Y. Brumer and G. M. Whitesides, *Nature Materials*, 2003, **2**, 241–245.

10 L. S. McCarty, A. Winkleman and G. M. Whitesides, *Journal of the American Chemical Society*, 2007, **129**, 4075–4088.
11 S. S. Kwak, S. Lin, J. H. Lee, H. Ryu, T. Y. Kim, H. Zhong, H. Chen and S.-W. Kim, *ACS Nano*, 2016, **10**, 7297–7302.
12 A. S. Aji, R. Nishi, H. Ago and Y. Ohno, *Nano Energy*, 2020, **68**, 104370.
13 C. Liu and A. J. Bard, *Chemical Physics Letters*, 2009, **480**, 145–156.
14 L. Tatar and H. Y. Kaptan, *Journal of Polymer Science Part B: Polymer Physics*, 1997, **35**, 2195–2200.
15 A. F. Diaz, D. Wollmann and D. Dreblow, *Chemistry of Materials*, 1991, **3**, 997–999.
16 T. A. de L. Burgo, C. A. Rezende, S. Bertazzo, A. Galembeck and F. Galembeck, *Journal of Electrostatics*, 2011, **69**, 401–409.
17 Z.-H. Lin, G. Cheng, L. Lin, S. Lee and Z. L. Wang, *Angewandte Chemie*, 2013, **125**, 12777–12781.
18 Z. L. Wang, T. Jiang and L. Xu, *Nano Energy*, 2017, **39**, 9–23.
19 W. Tang, B. D. Chen and Z. L. Wang, *Advanced Functional Materials*, 2019, **29**, 1901069.
20 P. Jiang, L. Zhang, H. Guo, C. Chen, C. Wu, S. Zhang and Z. L. Wang, *Advanced Materials*, 2019, **31**, 1902793.
21 A. Z. Stetten, D. S. Golovko, S. A. L. Weber and H.-J. Butt, *Soft Matter*, 2019, **15**, 8667–8679.
22 K. Yatsuzuka, Y. Mizuno and K. Asano, *Journal of Electrostatics*, 1994, **32**, 157–171.
23 A. F. Diaz and R. M. Felix-Navarro, *Journal of Electrostatics*, 2004, **62**, 277–290.
24 L. E. Helseth, *Journal of Electrostatics*, 2016, **81**, 64–70.
25 L. E. Helseth and H. Z. Wen, *European Journal of Physics*, 2017, **38**, 55804.
26 L. E. Helseth, *Langmuir*, 2019, **35**, 8268-8275,
27 L. E. Helseth, *Nano Energy*, 2020, **73**, 104809.
28 J. Park, Y. Yang, S.-H. Kwon and Y. S. Kim, *The Journal of Physical Chemistry Letters*, 2015, **6**, 745–749.
29 J. Park, S. Song, C. Shin, Y. Yang, S. A. L. Weber, E. Sim and Y. S. Kim, *Angewandte Chemie International Edition*, 2018, **57**, 2091–2095.
30 L.K.H. Van Beek, L. K. H. *Physica* 1960, **26**, 66-68.
31 G. M. Tsangaris, G. C. Psarras, N. Koulombi, *Journal of Materials Science*, 1998, **33**, 2027-2037.
32 X. Xia, Z. Zhong, G.J.Weng, *Mechanics of Materials*, 2017, **109**, 42–50.
33 F. Galembeck, T.A.L. Burgo. *Chemical Electrostatics: New Ideas on Electrostatic Charging: Mechanisms and Consequences*. Springer International Publishing AG 2017. ISBN 978-3-319-52373-6. ISBN 978-3-319-52374-3 (eBook). DOI 10.1007/978-3-319-52374-3
34 M. D. Sosa, G. Lombardo, G. Rojas, M. E. Oneto, R. M. Negri and N. B. D'Accorso, *Applied Surface Science*, 2019, **465**, 116–124.
35 L. Chen, F. Wu, Y. Li, Y. Wang, L. Si, K. I. Lee and B. Fei, *Journal of Membrane Science*, 2018, **547**, 93–98.
36 Shirtcliffe NJ, McHale G, Atherton S, Newton MI, An introduction to superhydrophobicity, Adv Colloid Interface Sci. 161 (2010). doi:10.1016/j.cis.2009.11.001.
37 A. L. Sumner, E. J. Menke, Y. Dubowski, J. T. Newberg, R. M. Penner, J. C. Hemminger, L. M. Wingen, T. Brauers and B. J. Finlayson-Pitts, *Physical Chemistry Chemical Physics*, 2004, **6**, 604.
38 C. J. Peacock, P. J. Hendra, H. A. Willis and M. E. A. Cudby, *Journal of the Chemical Society A: Inorganic, Physical, Theoretical*, 1970, 2943.
39 E. Németh, V. Albrecht, G. Schubert and F. Simon, *Journal of Electrostatics*, 2003, **58**, 3–16.
40 T. L. Tarbuck, S. T. Ota and G. L. Richmond, *Journal of the American Chemical Society*, 2006, **128**, 14519–14527.

41 A. G. Banpurkar, Y. Sawane, S. M. Wadhai, C. U. Murade, I. Siretanu, D. van den Ende and F. Mugele, *Faraday Discussions*, 2017, **199**, 29–47.
42 G. Beamson, D. Briggs, High Resolution XPS of Organic Polymers - The Scienta ESCA300Database Wiley Interscience, 1992
43 S. J. Kerber, J. J. Bruckner, K. Wozniak, S. Seal, S. Hardcastle and T. L. Barr, *Journal of Vacuum Science & Technology A: Vacuum, Surfaces, and Films*, 1996, **14**, 1314–1320.
44 B. J. Kirby and E. F. Hasselbrink, *ELECTROPHORESIS*, 2004, **25**, 187–202.
45 T. Preočanin, A. Selmani, P. Lindqvist-Reis, F. Heberling, N. Kallay and J. Lützenkirchen, *Colloids and Surfaces A: Physicochemical and Engineering Aspects*, 2012, **412**, 120–128.
46. A. Barišića, J. Lützenkirchen, G. Lefévre, T. Begović. Colloids and Surfaces A, 2019, **579**, 123616-123623.
47 N. Agmon, H. J. Bakker, R. K. Campen, R. H. Henchman, P. Pohl, S. Roke, M. Thämer and A. Hassanali, *Chemical Reviews*, 2016, **116**, 7642–7672.
48 V. Tandon and B. J. Kirby, *ELECTROPHORESIS*, 2008, **29**, 1102–1114.
49 J. K. Beattie, A. M. Djerdjev and G. G. Warr, *Faraday Discuss.*, 2009, **141**, 31–39.
50 A. Gray-Weale and J. K. Beattie, *Physical Chemistry Chemical Physics*, 2009, **11**, 10994.
51 K. N. Kudin and R. Car, *Journal of the American Chemical Society*, 2008, **130**, 3915–3919.
52 R.F. Gouveia, J.S. Bernardes, T.R. D. Ducati, F. Galembeck, *Analytical Chemistry*, 2012, **84**, 10191−10198
53 A. J. Bard and L. R. Faulkner, *Electrochemical methods: fundamentals and applications*, Wiley, New York, 2nd ed., 2001.
54 D.E. Yates, S. Levine, T.W. Healy, *Journal of the Chemical Society Faraday Transactions. I,* |1974, **70**, 1807-1818
55 Y. A. P. Sirkin, A. Hassanali and D. A. Scherlis, *The Journal of Physical Chemistry Letters*, 2018, **9**, 5029–5033.

View Article Online
DOI: 10.1039/D0SM00738B

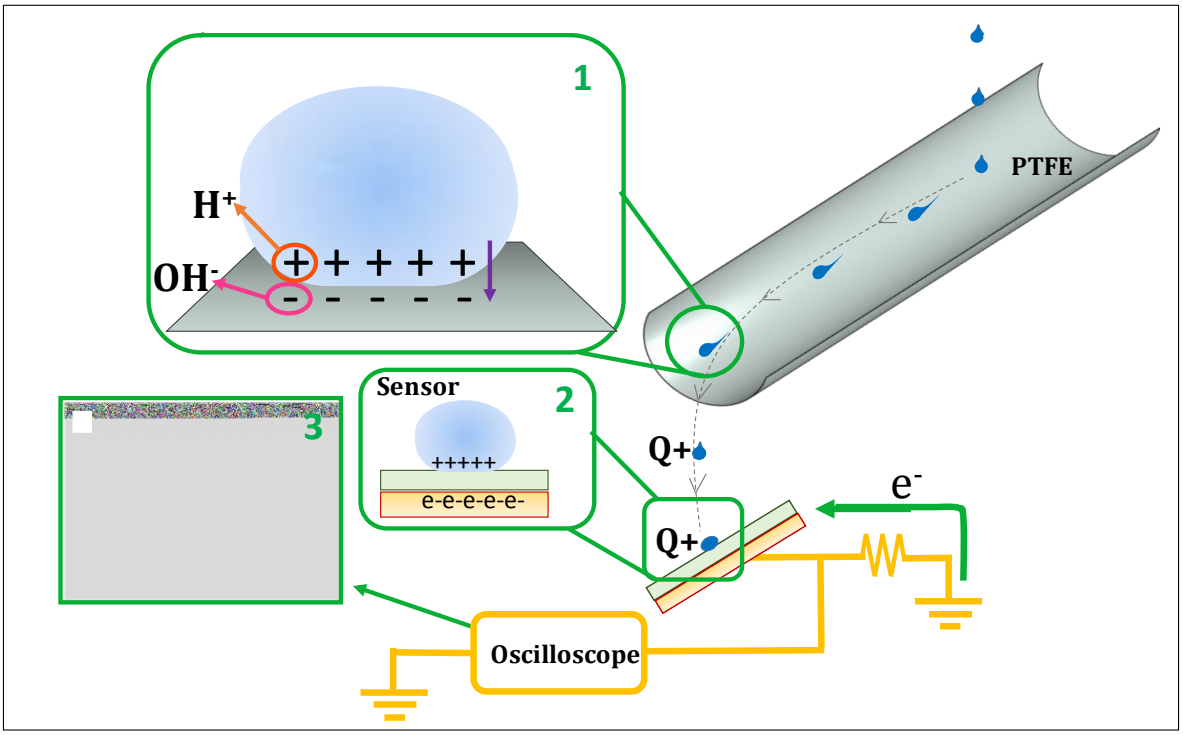

- **Water drops becomes charged after sliding on the polymer surface**
- **The variation of the detected charge, Q, with pH and Ionic Strength of the drop are compatible with OH^- or H^+ transfer from the drops to the polymer.**
- **A proposed thermodynamic model allows obtaining quantitative predictions of pH and Ionic Strength effects on the charge.**